THE JOURNAL OF BIOLOGICAL CHEMISTRY

A New Potent HIV-1 Reverse Transcriptase Inhibitor

A SYNTHETIC PEPTIDE DERIVED FROM THE INTERFACE SUBUNIT DOMAINS*

(Received for publication, April 23, 1999, and in revised form, May 24, 1999)

May C. Morris‡§, Veronique Robert-Hebmann¶, Laurent Chaloin‡§, Jean Mery‡, Frederic Heitz‡, Christian Devaux¶, Roger S. Goody‖, and Gilles Divita‡**

From the ‡Biophysics Department, Centre de Recherches de Biochimie Macromoléculaire, CNRS, 1919 Route de Mende, 34283 Montpellier, Cedex 5, France, ¶Laboratoire Infections Rétrovirales et Signalisation Cellulaire, CRBM-CNRS UPR1086, Institut de Biologie, 4, Boulevard Henri IV, 34060 Montpellier Cedex 1, France, and ‖Max Planck Institut fur Molekular Physiologie, Rheinlanddamm 201, 44139 Dortmund, Germany

The biologically relevant and active forms of human immunodeficiency viruses type 1 and 2 reverse transcriptase found in infectious virions are heterodimers produced in a two-step dimerization process. Dimerization involves first the rapid association of the two subunits, followed by a slow conformational change yielding a fully active form. We have shown that the dimeric nature of reverse transcriptase represents a important target for the design of a new class of antiviral agents. In this work, we propose a new strategy for its inhibition by targeting protein/protein interactions during viral formation in infected cells. From the screening of peptides derived from the tryptophan cluster at the interface of the connection subdomain, we have designed a short peptide (10 residues) corresponding to residues 395–404, which can block dimerization of reverse transcriptase *in vitro* and in infected cells. This peptide is highly efficient in abolishing the production of viral particles, without any adverse toxic side effects, when transduced into human immunodeficiency virus type 1-infected cells together with a new peptide carrier.

Reverse transcriptase (RT)[1] plays a key role in the replication of HIV by converting single-stranded genomic RNA into double-stranded proviral DNA and represents one of the main targets for the development of AIDS therapy. Most inhibitors of RT described in the past years, whether nucleoside analogues or nonnucleoside inhibitors target the polymerase activity of RT but present some limitations including toxicity and the emergence of resistant strains (1–3).

The biologically relevant and active form of human immunodeficiency virus reverse transcriptases (HIV-RT) found in infectious virions is a heterodimer containing two polypeptides, p66 and p51; the latter derived from the former by proteolytic cleavage of its C-terminal domain (4, 5). The structure of HIV-1 RT has been solved in different states: unliganded (6), complexed with nonnucleoside inhibitors (7–9), complexed with double-stranded DNA (10), and covalently trapped with DNA template/primer and deoxynucleoside triphosphate (11) and reveals an asymmetric interaction between the two subunits. The p66 and p51 subunits contain four similar subdomains forming the polymerase domain termed fingers, palm, thumb, and connection with a similar individual structure but a significantly different orientation relative to one another (6–8).

We have demonstrated that heterodimeric RTs are produced in a two-step dimerization process, which involves the rapid association of the two subunits into an inactive dimer, followed by a slow conformational change yielding the fully active form (12, 13). The dimer interface is mainly dominated by hydrophobic interactions between the two connection subdomains (13–15). Based on the x-ray crystallographic structure of HIV-1 RT, we have shown that the first interaction between p66 and p51 occurs in a Trp-rich hydrophobic cluster located in the connection subdomain of the two subunits and is followed by a conformational change that stacks the thumb subdomain of p51 onto the RNase-H domain of p66 and places the fingers subdomain of p51 in the palm subdomain of p66 (12).

An interesting feature of HIV-1 RT is that the dimeric form of the enzyme is absolutely required for all enzymatic activities (16–18). As such, we have proposed the dimerization process of RT as an interesting target for AIDS chemotherapy (16, 19, 20). In this work, we describe a new strategy for RT inhibition by targeting protein/protein interactions during viral formation in infected cells. We demonstrate that a short peptide (10 residues) derived from the tryptophan cluster at the interface of the connection subdomains inhibits dimerization of RT *in vitro* and abolishes the production of viral particles without any adverse toxic side effects when transduced into HIV-1 infected cells.

EXPERIMENTAL PROCEDURES

Peptide Synthesis—The different peptides were synthesized by solid phase peptide synthesis using aminoethyldithio-2-isobutyric acid-expensin resin with a 9050 Pepsynthetizer (Millipore, UK) according to the Fmoc(*N*-(9-fluorenyl)methoxycarbonyl)/*tert*-butyl method, purified by semi-preparative HPLC and identified by electrospray mass spectrometry and amino acid analysis (21, 22). To increase their stability, both peptides were acetylated at the N terminus and linked to a cysteamide group at the C-terminal part (22). For cellular localization, peptides were coupled with Lucifer yellow iodoacetamide dipotassium salt (Molecular Probes) (21).

Enzyme Preparation—Recombinant HIV-1 $_{BH10}$ RT was expressed in *Escherichia coli* and purified as described previously (17). Highly homogenous preparations of the heterodimeric form of the enzyme obtained by co-expressing the 66- and 51-kDa subunits were used. Enzyme concentration was routinely determined by Bradford (23) using gravimetrically prepared solutions of RT as a standard.

* This work was supported by the CNRS, and by grants from the Agence Nationale pour la Recherche sur le SIDA (ANRS), the Association pour la Recherche contre le Cancer (ARC), and the Fondation pour la Recherche Médicale (FRM) SIDACTION. The costs of publication of this article were defrayed in part by the payment of page charges. This article must therefore be hereby marked "*advertisement*" in accordance with 18 U.S.C. Section 1734 solely to indicate this fact.

§ Supported by fellowships from the ANRS.

** To whom correspondence should be addressed: Centre de Recherches de Biochimie Macromoléculaire, CNRS, 1919 Route de Mende, 34283 Montpellier, Cedex 5, France. Tel.: 33-04-67-61-33-92; Fax: 33-04-67-52-15-59; E-mail: gilles@puff.crbm.cnrs-mop.fr.

[1] The abbreviations used are: RT, reverse transcriptase; HIV, human immunodeficiency virus; HPLC, high pressure liquid chromatography; MOPS, 4-morpholinepropanesulfonic acid; MTT, 3-(4,5-dimethylthiazol-2-yl)-2,5-diphenyl tetrazolium bromide.

TABLE I

Inhibition of HIV-1 RT dimerization by synthetic peptides

All peptides were synthesized with cysteamide and acetyl groups at the C- and N-terminal end, respectively. Peptides 3, 4, 5, 6, 7, and 9 are soluble in water and the other peptides were solubilized in 10% Me_2SO. The effect of Me_2SO on the stability and polymerase activity of RT was shown to be less than 2% for the highest concentration of Me_2SO used. Association and activation rate constants were calculated from peptide concentration-dependent titration curves (Fig. 1), as a function of polymerase activity and of the degree of dimerization by HPLC size exclusion. The data reported here correspond to averages of four independent experiments.

Peptide sequences (HIV-1 BH_{10} isolate)	Association rate	Activation rate	K_d value
	$M^{-1}\ s^{-1}$	h^{-1}	μM
1. FKLPIQKETWETWWTEYWQATWYPEWEFV	$0.8\ 10^3$	0.05	1.2 ± 0.7
2. FKLPIQKETWETWWDNYWQVTW	$0.8\ 10^3$	0.047	1.5 ± 0.5
3. FKLPIQKETWETWWTEYWE	$1.5\ 10^3$	0.101	2.2 ± 0.9
4. FKLPIQKETWETWWTE	$1.05\ 10^3$	0.071	1.7 ± 0.2
5. KETWETWWDNYWQVTW	$0.21\ 10^3$	0.018	0.25 ± 0.1
6. KETWETWWTNYWE	$0.27\ 10^3$	0.012	0.34 ± 0.2
7. KETWETWWTE	$0.31\ 10^3$	0.018	0.24 ± 0.1
8. KETWETWWTEYWQATWYPEWE	$1.4\ 10^4$	0.12	65 ± 12
9. KETWETWWDNYWQVTWVPEWE	$0.9\ 10^4$	0.14	22 ± 6
10. TWWTEYWQATWYPEWEFV	$4.2\ 10^4$	0.16	>200
11. TEYWQATWIPEWE	$5.4\ 10^4$	0.18	
12. TEYWQATWIPEWEFV	$5.0\ 10^4$	0.18	

Polymerase RT Assay—Polymerase activity was measured in standard assays using poly(rA)-$(dT)_{15}$ as a primer/template as described previously (16). The RT preparations used showed a specific activity of about 10,000 units/mg, where 1 unit of enzyme catalyzes the incorporation of 1 nmol of TMP in 10 min at 37 °C into acid-insoluble materials.

HPLC Size Exclusion Chromatography—Chromatography was performed as already described (16, 19) using two HPLC columns in series (Bio-Rad TSK-125 and TSK-250). Size exclusion chromatography was performed with 5–10 μg of protein, and the columns were eluted with 200 mM potassium phosphate (pH 7.0) at a flow rate of 0.8 ml/min.

In Vitro RT Dimerization Assay—Dissociation of HIV-1 RT was achieved by addition of 17% acetonitrile into a 50 mM MOPS-HCl, pH 7.5 buffer containing 10 mM $MgCl_2$, 50 mM KCl, and 5% glycerol. Association of the subunits was then initiated in the absence or in the presence of increasing concentrations of peptides by a 12-fold dilution into an acetonitrile-free buffer resulting in a final concentration of 1.4% acetonitrile. All experiments were performed at 25 °C, with an enzyme concentration of 0.2–2 μM. Establishment of the dimerization equilibrium was followed in a time-dependent manner by size exclusion HPLC and polymerase activity assays using 100 ng of RT (16, 19). The kinetics of formation of native RT were measured with a 50-ng sample of RT for 5 min only at 37 °C, so as to limit any further activation by dimerization.

Cell Culture—Adherent human HS-68 fibroblasts as well as human MT4 and CEM-SS lymphoblasts in suspension were cultured in Dulbecco's modified Eagle's medium supplemented with 1% 200 mM glutamine, 1% antibiotics (streptomycin 10,000 μg/ml, penicillin 10,000 IU/ml) and 10% (w/v) fetal calf serum, at 37 °C in a humidified atmosphere containing 5% CO_2 as described previously (22). For investigating the cellular localization of peptides, cells were plated on glass coverslips and grown to 75% confluency, then overlaid with peptide or MPG-peptide complexes (ratio 20/1) and incubated for various times. The coverslips were then rinsed extensively with phosphate-buffered saline and cells were fixed in 2% paraformaldehyde for 5 min, then rehydrated in phosphate-buffered saline. Fluorescent images were shot using a Nikon camera directly connected to a personal computer. The cytotoxicity of both p7 and p7-MPG complexes were investigated in the cell lines mentioned above. Cells grown in 35-mm diameter dishes to 75% confluency ($0.5–1.10^6$ cells/dish) were incubated with 0.1 μM to 1 mM p7 alone or complexed to MPG in a 1/20 ratio. Cell culture medium with p7 or p7-MPG was not changed, and cell proliferation was measured over 4 days. Cytotoxicity was evaluated with the colorimetric 3-(4,5-dimethylthiazol-2-yl)-2,5-diphenyl tetrazolium bromide (MTT) assay, after removing cell culture medium and replacing it with phosphate-buffered saline containing 5 mg/ml of MTT (24).

Antiviral Activity—The CD4+ lymphoblastoid CEM cell line was obtained from the American Type Culture Collection (ATCC). Cells were cultured in RPMI 1640 medium supplemented with 10% fetal calf serum, 1% glutamax, and 1% penicillin-streptomycin antibiotic mixture (Life Technologies, Inc.) to a density of 5×10^5 cells/ml in a 5% CO_2 atmosphere. For infection, 10^6 CEM cells were incubated for 30 min at 4 °C with 100 μl of HIV-1_{LAI} at a concentration of $100 \times 50\%$ tissue culture infective dose. Then cells were washed five times and cultured at 5×10^5 cells/ml in 24-well microplates with various concentrations of peptide p7 and MPG-p7 (1 μM to 0.1 nM), 13B8.2 (66 nM) an anti-CD4 monoclonal antibody (Immunotech), or azidothymidine (10 μM). Viral production was monitored twice a week by measuring reverse transcriptase activity in 1 ml of cell-free supernatant.

Fluorescence Experiments—Fluorescence measurements were performed at 25 °C, using a Spex Fluorolog II Jobin Yvon fluorimeter. The fluorescence of peptides (0.5–1 μM) was measured in a total volume of 0.7 ml of buffer containing 50 mM Tris-HCl, 50 nM KCl, pH 7.5. Excitation was routinely performed at 290 nm, and fluorescence emission intensity was monitored at 340 nm. Titration curves were fitted using a quadratic equation with the Grafit program, as already described (22).

RESULTS AND DISCUSSION

Peptide Design—Based on the knowledge of both the dimerization process and the different x-ray structures of HIV-1 RT, the main interface between p66 and p51 subunits has been shown to involve a cluster of Trp residues in the two connection subdomains (20, 25–27). This cluster forms a hydrophobic patch in the region containing α-helix L and β-strand 19, (residues 389 to 422 in the BH_{10} isolate) (14, 15, 25). We have previously demonstrated that a peptide encompassing residues 388 to 415, in the connection domain can block the dimerization of HIV-1 and HIV-2 RTs *in vitro* (19, 20). To define a minimal sequence required for the inhibition of RT dimerization and to propose it as a new "antiviral-drug" for infected cells, 12 peptides (sequences are reported in Table I) derived from this interface domain were designed and synthesized with an acetylated N terminus and a C-terminal cysteamide group (21). These groups were added to increase the stability of the peptides and to improve their delivery into cells. Moreover the cysteamide group was useful for the covalent attachment of a fluorescent probe, allowing to investigate the cellular localization of the peptides.

Peptides Derived from the Connection Domain Inhibit RT Dimerization in Vitro—The potential of each peptide to inhibit RT *in vitro* was investigated. Dissociation of RT was performed at 25 °C by addition of 17% acetonitrile, and re-association of the subunits was induced by a 12-fold dilution of the sample into an acetonitrile-free buffer. The association rate of the subunits was determined by monitoring the ratio of dimeric RT by HPLC size exclusion (Fig. 1*a*), and the activation rate of dimeric RT was followed by measuring the recovery of polymerase activity of HIV-1 RT (Fig. 1*b*). Association and activation rates of HIV-1 RT in the absence of peptide inhibitors were calculated as $5.1\ 10^4\ M^{-1}\ s^{-1}$ and $0.17\ h^{-1}$, respectively. The presence of 5 μM of the 29-mer peptide (p1) corresponding to the α-helix L and β-strand 19 of the connection domain, strongly reduced both the association and activation rate constants to $0.8\ 10^3\ M^{-1}\ s^{-1}$ and $0.05\ h^{-1}$, respectively. As reported in Table I, most of the peptides derived from the Trp cluster of the

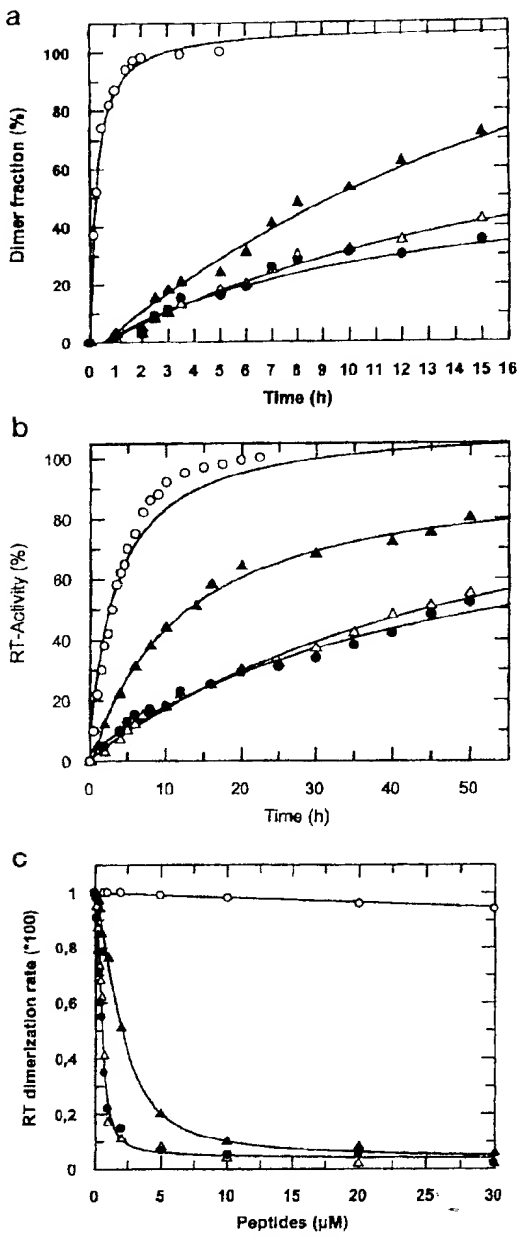

FIG. 1. **Peptide inhibition of HIV-1 RT dimerization process *in vitro*.** Heterodimeric RT (5 μM) was first dissociated with 17% of acetonitrile at pH 7.5, 25 °C, and monomer-monomer association was initiated by a 12-fold dilution in an acetonitrile-free buffer in the absence (○) or presence of 10 μM of peptide p1 (▲), p6 (△), and p7 (●). *a*, inhibition of HIV-RT dimerization by the different peptides was monitored by following the kinetics of monomer-monomer association by HPLC size exclusion chromatography with 10-μg samples of RT, and the data were analyzed according to a second-order reaction. *b*, inhibition by the different peptides was monitored by following the kinetics of formation of active heterodimeric RT, quantified in a polymerase activity assay. Curves were fitted as a single exponential. *c*, dependence of the dimerization rate constant of HIV-1 RT on peptide concentration. Monomer-monomer association was performed in the presence of increasing concentrations of p11 (○), p1 (▲), p6 (△), and p7 (●) peptides. Dimerization rate constants were determined by fitting the time-dependent association curve obtained by size exclusion HPLC as a second-order reaction.

connection subdomain affected both the association and the activation rates of heterodimeric HIV-1 RT. This correlation between polymerase activity and dimer formation reveals that lack of activity is due to the direct targeting by these peptides of the first step of the dimerization process of RT: monomer/monomer association. Peptides p5 (395–410), p6 (395–407), and p7 (395–404) corresponding to the N-terminal sequence of the Trp cluster were most efficient, reducing the association and activation rate constants of RT to 0.31–0.21 10^3 M^{-1} s^{-1} and 0.018–0.012 h^{-1}, respectively at 5 μM. That these shorter peptides should be at least 3-fold more efficient than longer peptides (p1 and p3) is probably due to their lack of folding, whereas p1 and p3 tend to fold into an α-helix and aggregate in solution.

In all cases, the association rate of HIV-1 RT is dependent on the concentration of peptide used. The titration curves obtained for p1, p6, and p7 reveal that these peptides exhibit a relatively high affinity for the two subunits of RT with overall K_d values of 1.2, 0.25, and 0.34 μM, respectively (Fig. 1*c*). In contrast, the lack of inhibition observed with peptides p11 and p12 suggests that the C-terminal part of the Trp cluster is not essential for the inhibition of RT dimerization. Finally the very low inhibition obtained with p10 confirms the essential role of Trp^{398} within the cluster, which is not surprising if one considers that in the structure of HIV-1 RT, residues "KETWET" within α-helix L forms the main contact at the p66/p51 interface (Fig. 2*b*). Moreover, mutation of Trp^{398} and Trp^{401} (in the $HIV\text{-}1_{BH10}$ isolate) strongly affected the stability of the dimeric form of HIV-1 RT *in vitro*.[2] However, this short sequence was not sufficient for inhibition of RT dimerization. Indeed, peptide p7, corresponding to full α-helix L, is the minimal sequence required to inhibit dimerization of RT *in vitro*. Based on these data we propose the minimal 10-residue peptide, KETWETWWTE, as an inhibitor of RT dimerization.

Cell Delivery of the Peptide Inhibitor—We further investigated the delivery of peptide p7 into cells and its antiviral activity on infected cell lines. The main problems in the delivery of drugs into cells are crossing the cell membrane and reaching the target within the cell. To locate peptides in different cell lines, we exploited the inherent properties of the cysteamide group at the C-terminal end of the peptide to covalently link a fluorescent probe, Lucifer yellow. Peptide 7 was applied onto cultured human adherent HS-68 fibroblasts in the presence of 10% serum. In these conditions no degradation of the peptides could be detected after 1 h incubation. As shown in Fig. 3, peptide inhibitors entered cells poorly and after 1 h of incubation, localized in the cytoplasm (Fig. 3*b*). To overcome the lack of efficient cell delivery, we used a carrier peptidyl system (MPG) derived from the fusion peptide of gp41 and containing the nuclear localization sequence of SV40 large T antigen (22). This bifunctional carrier contains a hydrophobic N-terminal domain and a hydrophilic C-terminal moiety, the latter being extremely powerful for the delivery of oligonucleotides and plasmids into cells (22). Here we used the hydrophobic domain of this carrier to form contacts with the anti-RT peptides.

Binding of p7 to MPG was determined by measuring changes in the intrinsic Trp fluorescence of the peptide, upon titration of a fixed concentration of MPG (1 μM) with increasing concentrations of p7. The corresponding titration curve (Fig. 3*e*), reveals that p7 interacts strongly with MPG, induces an important quenching of fluorescence up to 30%, with a dissociation constant of approximately 30 ± 7 nM. The fluorescence of MPG should be negligible compared with that of p7, which contains 3 Trp residues. The quenching of fluorescence of MPG observed, suggests that the fluorescence of p7 is completely abolished upon binding to MPG. Saturation takes place for a con-

[2] M. C. Morris and G. Divita, unpublished results.

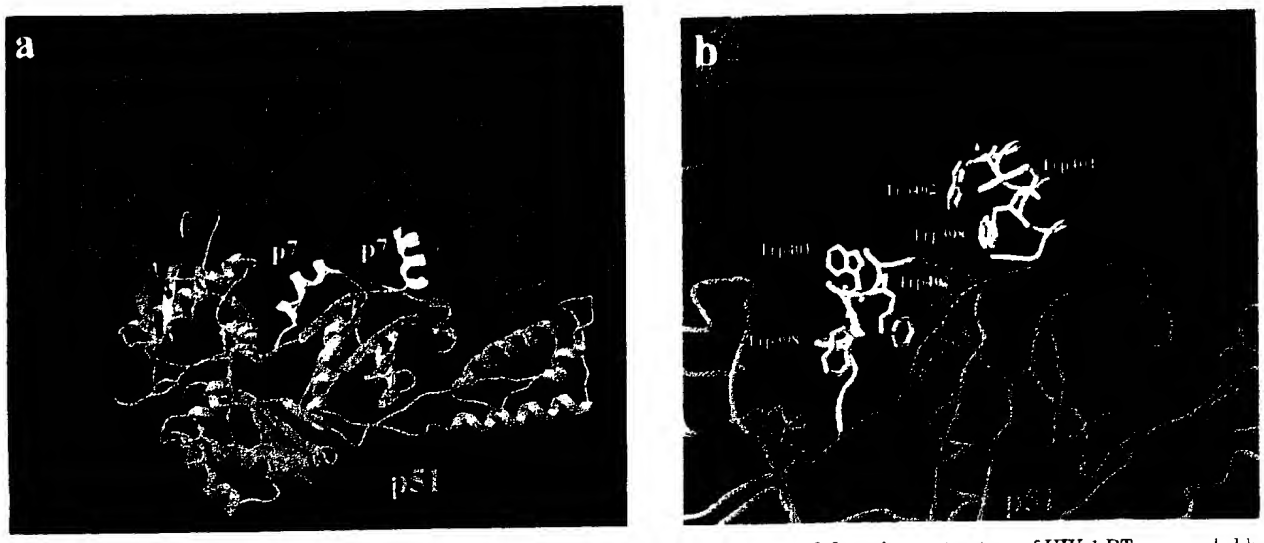

FIG. 2. **Structure of HIV-1 RT and location of the Trp cluster in the connection subdomain.** *a*, structure of HIV-1 RT as revealed by x-ray crystallography (6–11). p51 and p66 subunits are in *green* and *red*, respectively. The structures of p7 in p66 and p51 are shown in *white*. *b*, location of the Trp^{398}, Trp^{401}, and Trp^{402} in the thumb subdomain interface between p66 and p51.

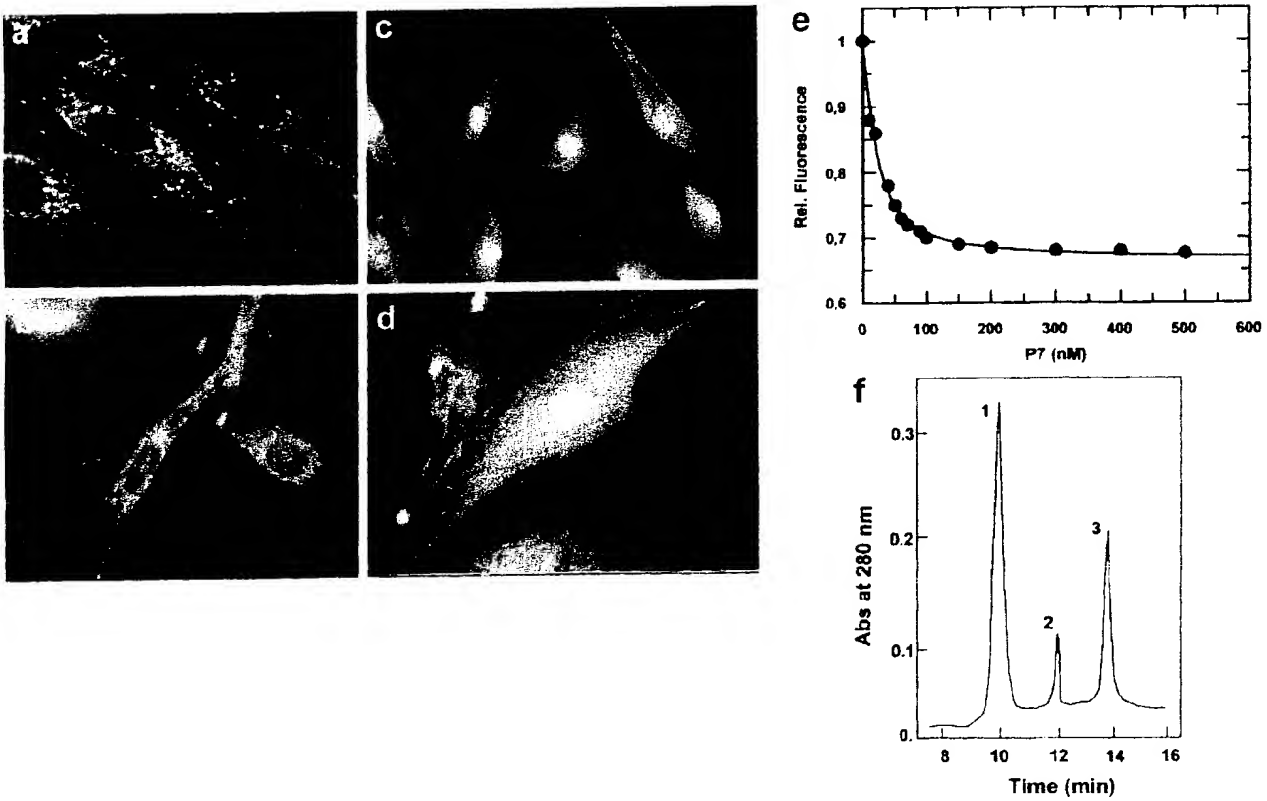

FIG. 3. **Formation, cellular localization, and cell delivery of MPG-p7 complex.** Peptides and complexes were applied onto HS68 plated on glass coverslips and grown to 75% confluency in the presence of 10% serum. The cellular localization of p7, and of the MPG-P7 complex (ratio 1/20) was monitored by confocal microscopy thanks to C-terminally fluorescently labeled peptide. *a*, control experiment with free Lucifer yellow; *b*, 1 μM of p7 in the absence of MPG; *c* and *d*, 0.1 μM of p7-MPG complex incubated for 30 min and 5 min, respectively, before fixation and observation; *e*, the formation of the MPG-p7 complex was monitored by measuring changes in intrinsic tryptophan fluorescence of MPG at 340 nm, upon excitation at 290 nm. A fixed concentration of MPG (1 μM) was titrated with increasing amounts of p7; *f*, the different populations of p7 and p7-MPG complexes were purified by size exclusion HPLC. MPG (5 μM) and p7 (0.1 μM) were incubated for 15 min in phosphate buffer, pH 7.0, then applied onto a size exclusion HPLC column (TSK 125, Bio-Rad 7, 5 × 300 mm) and eluted with 200 mM potassium phosphate, pH 7.0, at a flow rate of 1.0 ml/min.

centration of p7 of 50 nM, which is 20-fold lower than that of the MPG, suggesting that p7 interacts strongly with more than one molecule of MPG. From the K_d and the saturation concentration values we estimated the ratio to 30 molecules of MPG for one molecule of peptide inhibitor.

The preformed MPG-p7 complex was separated and purified

by size exclusion HPLC in a high concentration of salt (200 mM NaCl). Three different subpopulations were observed (Fig. 3*f*): the main peak (1) corresponding to a molecular mass of ~50 kDa, which can be assessed as a complex of p7-MPG at a 1/20 ratio, when taking into account the molecular weight of each peptide (2.4 kDa for MPG and 0.8 kDa for p7); peaks 2 and 3 correspond to lower molecular weight complexes (20 kDa) containing both MPG and p7 and to the monomeric form of MPG, respectively. No monomeric p7 was detected, suggesting that in these conditions all p7 is complexed with MPG. The stability of the p7-MPG complex in high salt concentrations and the presence of hydrophobic residues in the sequence of p7 favor the notion of a hydrophobic interaction between the two peptides. Moreover the interaction between p7 and MPG promotes further MPG/MPG interactions, leading to the formation of a peptide carrier cage around p7. The main contacts between MPG and anti-RT peptides may involve the fusion sequence of gp41 and the Trp cluster.

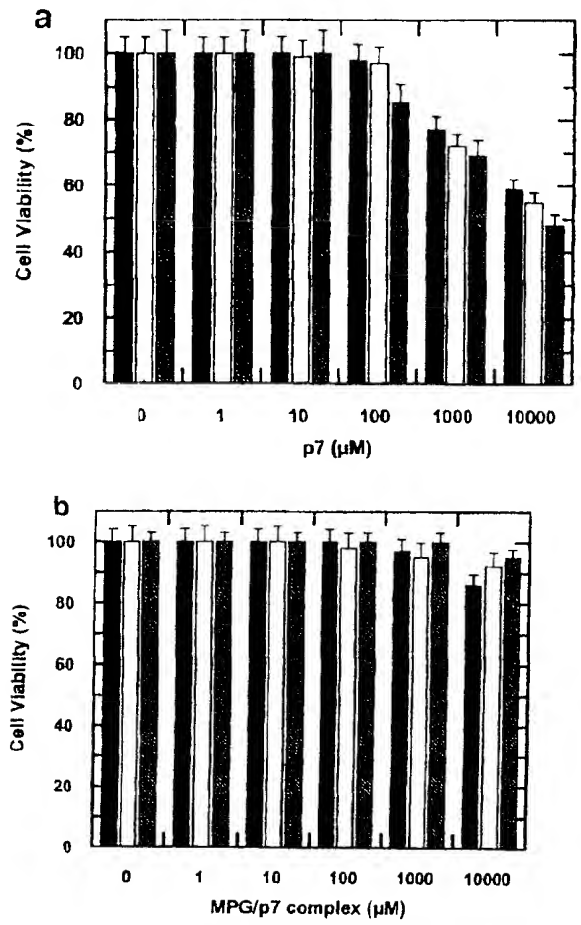

FIG. 4. **Cytotoxicity of p7 and MPG-p7 complex.** The toxicity of p7 (*panel a*) and of the p7-MPG complex (ratio 20/1) (*panel b*) were monitored in different cell lines including HS68 (■), MT4 (□), and CEM-SS (▨) cells. Cell death was quantified by MTT staining after 2 days of incubation.

The high molecular weight p7-MPG complex was purified and both its cellular localization and antiviral activity were analyzed. When complexed at a 20/1 ratio with MPG, p7 localized rapidly in the cytoplasm in less than 5 min, but after 30 min could be found mainly in the nucleus (Fig. 3, *c* and *d*). In contrast when complexed with MPG at a 10/1 ratio, most of p7 was retained in the cell membranes, suggesting that this complex is not stable enough in the cell culture medium. Hence, formation of a large particle seems to improve the stability of p7 and to increase its delivery into cells.

Toxicity of the Peptide Inhibitor—The degree of toxicity of p7 and of the MPG/p7 (20/1) complex were analyzed in different cell lines, including HS-68, MT-4, and CEM-SS cell lines. No toxicity was observed for concentrations of p7 up to 10 μM, and cell viability was only decreased by about 5–10%, depending on the cell line, for a peptide concentration of 100 μM (Fig. 4*a*). We have already reported that MPG alone is not toxic at concentrations up to 100 μM (19); when complexed with p7, no cytoxicity was observed for concentrations up to 1 mM (Fig. 4*b*), which is much higher than the concentration required for inhibition of HIV-1 RT by p7 *in vitro* or than the K_d value of this peptide for the subunits of RT. In conclusion, the interaction between p7 and MPG, decreases toxicity and improves cell delivery of the peptide.

Antiviral Activity of the Peptide Inhibitor—The ability of p7 and of the p7-MPG complex to inhibit HIV-1 infection in cultured CEM-T cells was measured by monitoring RT activity in

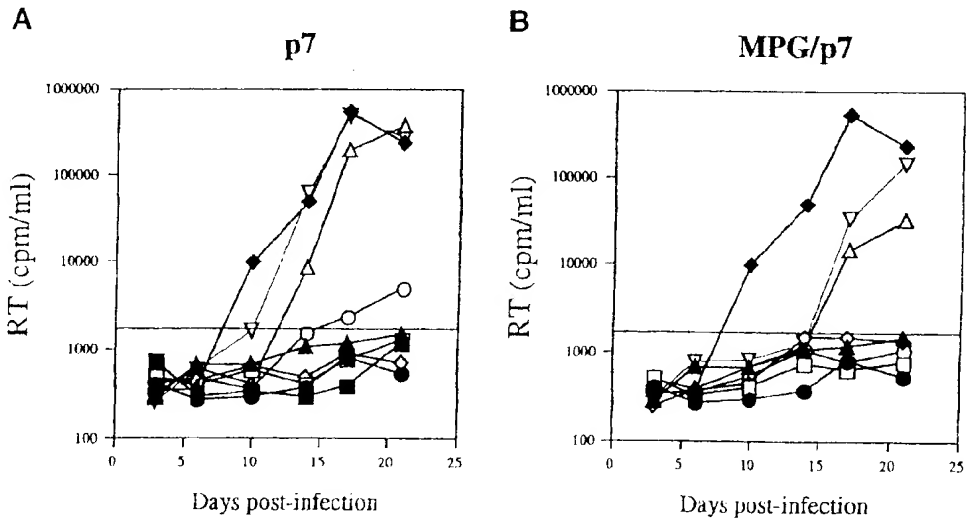

FIG. 5. **Effect of different concentrations of p7 and MPG-p7 on HIV-1 infection.** CEM cells exposed to 100 μl of viral suspension containing 100 × 50% tissue culture infective dose of HIV-1_{LAI} were cultured in medium alone (◆), medium-supplemented with 13B8.2 (66 nM) (●), azidothymidine (10 μM) (▲), peptide 7 (*panel a*) or MPG-p7 (*panel b*) at 1 μM (□), 100 nM (◇), 10 nM (○), 1 nM (△), and 0.1 nM (▽). Viral production was monitored by measuring RT activity. Culture supernatants from virus-free CEM cells (■) were tested as a control.

the cell-free culture supernatants. The peptides were added after a 30-min adsorption of the virus at 4 °C, just before incubation of the cells at 37 °C. Kinetics of HIV-1 production in the presence of p7 or of MPG-p7 are reported in Fig. 5. We investigated the kinetics of viral production in the presence of different concentrations of p7 and MPG/p7, in comparison with two other HIV inhibitors: azidothymidine (10 μM) and anti-CD4 antibody 13B8.2 (66 nM) (28). In the presence of 100 nM of p7 no virus was detected up to 22 days post-infection (Fig. 5*a*). For a concentration of 10 nM of p7, viral replication was inhibited during the first 15 days, after which slow propagation of virus was detected in the RT assay and confirmed by dosage of p24 (data not shown). For lower concentrations of p7 (1 and 0.1 nM), viral production was slightly delayed compared with the control without inhibitor. When p7 was complexed to MPG, antiviral activity was markedly improved, as no virus was detected 22 days after infection with 10 nM of p7 (Fig. 5*b*). Even at the lowest concentration used (0.1 nM), no virus was detected up to 15 days post-infection. That no virus was detected after at least 1 month at higher concentrations of p7·MPG complex (100 nM), suggests that the viral production observed at low concentrations of p7 is mainly due to the limitation of p7 and not to a resistant mutation in RT. The p7·MPG complex is therefore at least 10-fold more efficient than p7, probably due to the fact that MPG enhances both cell delivery and stability of the antiviral peptide in cell culture medium.

CONCLUSION

The antiviral properties of a peptide derived from the connection domain of RT validate the concept that dimerization of RT is an excellent target for the design of new HIV inhibitors. From our results, we conclude that peptide p7 is a very promising antiviral agent for many reasons. (a) p7·MPG complex strongly inhibits HIV-1 production in infected cells and can be used at a very low concentration (1 nM), without any adverse toxic side effects. (b) The sequence of p7 KETWETWWTE is well conserved in all isolates of HIV-1and HIV-2 and is not reported in other proteins except reverse transcriptases (12, 20, 25), suggesting that the Trp cluster is a natural key domain involved in the formation of active RT and that such a peptide can be used as a highly specific inhibitor of both HIV-1 and HIV-2. (c) p7 being a short peptide (10 residues) has proven extremely important for its development as a new antiviral drug, as shortness improves both its stability in cell culture medium and its potency against AIDS.

Two hypotheses, which are not mutually exclusive, can be proposed to explain the mechanism through which RT activity is inhibited by these peptides in infected cells: peptides may block the formation of active RT before budding of the virus during the last step of the viral cycle and/or may also inhibit the first step of infection by inducing the dissociation of a preformed RT dimer required for reverse transcription. That heterodimeric RT is extremely stable and difficult to dissociate *in vitro* (13) favors the model of inhibition of the formation of active RT. The nature of the *in vivo* pathway of RT activation is not yet clear, but may require first an association leading to p66/p66 homodimer, followed by the proteolytic cleavage of one of the RNase-H domains by HIV protease (4, 5); the interaction between the thumb domain of p51 and the RNase H domain of p66 may then take place to yield mature heterodimeric RT. The important antiviral activity of p7 observed at a concentration 100-fold lower than the K_d value measured *in vitro* between p7 and RT subunits (0.24 μM), suggests that *in vivo* subunit association is directly controlled by the connection subdomains and that p7 may also interfere with the conversion of the p66/p66 homodimer into a p51/p66 heterodimer.

Acknowledgments—We thank Katrin Rittinger, Tobias Restle, and Jean Baillon for helpful discussions and Marcel Dorée for encouragement and support.

REFERENCES

1. Richman, D. D. (1996) *Adv. Exp. Med. Biol.* **394,** 383–395
2. Erickson, J. W., and Burt, K. S. (1996) *Annu. Rev. Pharmacol. Toxicol.* **36,** 545–571
3. Goody R. S. (1995) *Nat. Med.* **6,** 519–520
4. Di Marzo Veronese, F., Copeland, T. D., De Vico, A. L., Rahman, R., Oroszlan, S., Gallo, M., and Sarngadharan, M. G. (1986) *Science* **231,** 1289–1291
5. Lightfoote, M. M., Colligan, J. E., Folks, T. M., Fauci, A. S., Martin, M. A., and Venkatesan, S. (1986) *J. Virol.* **60,** 771–775
6. Rodgers, D. W., Gamblin, S. J., Harris, B. A., Ray, S., Culp, J. S., Hellmig, B., Woolf, D. J., Debouck, C., and Harrison, S. C. (1995) *Proc. Natl. Acad. Sci. U. S. A.* **92,** 1222–1226
7. Kohlstaedt, L. A., Wang, J., Friedman, J. M., Rice, P. A., and Steitz, T. A. (1992) *Science* **256,** 1783–1790
8. Esnouf, R., Ren, J., Ross, C., Jones, Y., Stammers, D., and Stuart, D. (1995) *Nat. Struct. Biol.* **2,** 303–308
9. Ren, J., Esnouf, R., Garman, E., Somers, D., Ross, C., Kirby, I., Keeling, J., Darby, G., Jones, Y., Stuart, D., and Stammers, D. (1995) *Nat. Struct. Biol.* **2,** 293–302
10. Jacobo-Molina, A., Ding, J., Nanni, R. G., Clark, A. D., Jr., Lu, X., Tantillo, C., Williams, R. L., Kamer, G., Ferris, A. L., Clark, P., Hizi, A., Hughes, S. H., and Arnold, E. (1993) *Proc. Natl. Acad. Sci. U. S. A.* **90,** 6320–6324
11. Huang, H., Chopra, R., Verdine, G. L., and Harrison, S. C. (1998) *Science* **282,** 1669–1675
12. Divita, G., Rittinger, K., Geourjon, C., Deleage, G., and Goody, R. S (1995) *J. Mol. Biol.* **245,** 508–521
13. Divita, G., Rittinger, K., Restle, T., Immendorfer, U., and Goody, R. S. (1995) *Biochemistry* **34,** 16337–16346
14. Wang, J., Smerdon, S. J., Jäger, J., Kohlstaedt, L. A., Rice, P. A., Friedman, J. M., and Steitz, T. A. (1994) *Proc. Natl. Acad. Sci. U. S. A.* **91,** 7242–7246
15. Becerra, S. P., Kumar, A., Lewis, M. S., Widen, S. G., Abbotts, J., Karawya, E. M., Hughes, S. H., Shiloach, J., and Wilson, S. H. (1991) *Biochemistry* **30,** 11707–11719
16. Restle, T., Muller, B., and Goody, R. S. (1990) *J. Biol. Chem.* **265,** 8986–8988
17. Muller, B., Restle, T., Weiss, S., Gautel, M., Sczakiel, G., and Goody, R. S. (1989) *J. Biol. Chem.* **264,** 13975–13978
18. Restle, T., Müller, B., and Goody, R. S. (1992) *FEBS Lett.* **300,** 97–100
19. Divita, G., Baillon, J. G., Rittinger, K., Chermann, J. C., and Goody, R. S. (1995) *J. Biol. Chem.* **270,** 28642–28646
20. Divita, G, Restle, T., Goody, RS., Chermann, JC., and Baillon, J. G. (1994) *J. Biol. Chem.* **269,** 13080–13083
21. Mery, J., Granier, C., Juin, M., and Brugidou, J. (1993) *Int. J. Pept. Protein Res.* **42,** 44–52
22. Morris, M. C., Vidal, P., Chaloin, L., Heitz, F., and Divita G. (1997) *Nucleic Acids Res.* **25,** 2730–2736
23. Bradford, M. (1976) *Anal. Biochem.* **72,** 248–254
24. Mosmann, T. (1983) *J. Immunol. Methods* **65,** 55–63
25. Baillon, J. G., Nashed, N. T., Kumar, A., Wilson, S. H., and Jerina, D. M. (1991) *New Biol.* **3,** 1015–1029
26. Debyser, Z., and De Clercq, E. (1996) *Protein Sci.* **5,** 278–286
27. Jacques, P. S., Wöhrl, B. M., Howard, K. J., and Le Grice, S. (1994) *J. Biol. Chem.* **269,** 1388–1393
28. Benkirane, M., Corbeau, P., Housset, V., and Devaux, C. (1993) *EMBO J.* **12,** 4909–4921